Geochemistry Geophysics Geosystems G3
AN ELECTRONIC JOURNAL OF THE EARTH SCIENCES
Published by AGU and the Geochemical Society

Technical Brief
Volume 7, Number 5
10 May 2006
Q05009, doi:10.1029/2005GC001100
ISSN: 1525-2027

U-Pb dating of zircon by LA-ICP-MS

Zhaoshan Chang
Department of Geology, Washington State University, Pullman, Washington 99164-2812, USA

Now at Centre of Excellence in Ore Deposits (CODES), University of Tasmania, Private Bag 79, Hobart 7001, Tasmania, Australia (zhaoshan.chang@utas.edu.au)

Jeffery D. Vervoort
Department of Geology, Washington State University, Pullman, Washington 99164-2812, USA

William C. McClelland
Department of Geological Sciences, University of Idaho, Moscow, Idaho 83844-3022, USA

Charles Knaack
Department of Geology, Washington State University, Pullman, Washington 99164-2812, USA

[1] In this study we used LA-ICP-MS (laser ablation–inductively coupled plasma–mass spectrometry) to determine U-Pb ages of 5 zircon samples of known age (~1800 Ma to ~50 Ma) in order to determine the reproducibility, precision, and accuracy of this geochronologic technique. This work was performed using a ThermoFinnigan Element2 magnetic sector double-focusing ICP-MS coupled with a New Wave Research UP-213 laser system. The laser ablation pit sizes ranged from 30 to 40 μm in diameter. Laser-induced time-dependent fractionation is corrected by normalizing measured ratios in both standards and samples to the beginning of the analysis using the intercept method. Static fractionation, including those caused during laser ablation and due to instrumental discrimination, is corrected using external zircon standards. Total uncertainty for each laser analysis of an unknown is combined quadratically from the uncertainty in the measured isotope ratios of the unknown and the uncertainty in the fractionation factors calculated from the measurement of standards. For individual analyses we estimate that the accuracy and precision are better than 4% at the 2 sigma level, with the largest contribution in uncertainty from the measurement of the standards. Accuracy of age determinations in this study is on the order of 1% on the basis of comparing the weighted average of the LA-ICP-MS determinations to the TIMS ages. Due to unresolved contributions to uncertainty from the lack of a common Pb correction and from potential matrix effects between standards and unknowns, however, this estimate cannot be universally applied to all unknowns. Nevertheless, the results of this study provide an example of the type of precision and accuracy that may be possible with this technique under ideal conditions. In summary, the laser ablation technique, using a magnetic sector ICP-MS, can be used for the U-Pb dating of zircons with a wide range of ages and is a useful complement to the established TIMS and SHRIMP techniques. This technique is especially well suited to reconnaissance geochronologic and detrital zircon studies.

Components: 10,510 words, 6 figures, 5 tables.

Keywords: laser ablation; magnetic sector ICP-MS; U-Pb dating; zircon dating.

Index Terms: 1115 Geochronology: Radioisotope geochronology; 1194 Geochronology: Instruments and techniques.

Received 3 August 2005; **Revised** 4 February 2006; **Accepted** 13 March 2006; **Published** 10 May 2006.

Chang, Z., J. D. Vervoort, W. C. McClelland, and C. Knaack (2006), U-Pb dating of zircon by LA-ICP-MS, *Geochem. Geophys. Geosyst.*, *7*, Q05009, doi:10.1029/2005GC001100.

1. Introduction

[2] The ability of LA-ICP-MS (laser ablation–inductively coupled plasma–mass spectrometry) to determine U-Pb zircon ages with reasonable accuracy and precision has been demonstrated by a number of laboratories over the past decade [*Feng et al.*, 1993; *Fryer et al.*, 1993; *Hirata and Nesbitt*, 1995; *Horn et al.*, 2000; *Li et al.*, 2000, 2001; *Kosler et al.*, 2002; *Jeffries et al.*, 2003; *Tiepolo*, 2003], enabling this technique to gain acceptance as a complementary geochronological tool to established methods using TIMS (Thermal Ionization Mass Spectrometer) and SHRIMP (Sensitive High Resolution Ion Microprobe). The advantages of the LA-ICP-MS technique are its short analytical time, moderate spatial resolution, and relatively low cost, allowing it to be useful for detrital zircon work and reconnaissance geochronologic studies.

[3] Uncertainty produced during LA-ICP-MS analyses comes from multiple sources. Each of these uncertainties needs to be incorporated into the final error assignment but several are difficult to quantify. In particular, the uncertainty introduced by matrix effects between the different zircons [*Black*, 2005] remains problematic. Nevertheless, it is important to arrive at a reasonable error estimate for each analysis in applications such as detrital zircon studies where each age determination needs to be a stand-alone result. Realistic reporting of the precision and accuracy of the LA-ICP-MS U-Pb age determinations is needed to integrate results from this method with those from the established TIMS and SHRIMP methods.

[4] The method for U-Pb data collection, error assessment, and age calculation currently employed at the LA-ICP-MS geochronology facility at Washington State University is outlined below. This technique has its roots and remains similar to an initial method developed in conjunction with George Gehrels at the University of Arizona, which has been used in a number of papers [e.g., *Dickinson and Gehrels*, 2003]. The present study demonstrates that, under ideal conditions, LA-ICP-MS U-Pb zircon geochronology is capable of accuracy and precision on the order of 2–4% (two sigma) on the basis of the comparison of LA-ICP-MS determinations to TIMS ages for the Cenozoic to Paleoproterozoic samples reported here. For single analyses, we estimate precision and accuracy of the age determinations to be better than 4%. Improvements in precision and accuracy can be achieved with development of zircon standards that are homogenous, concordant, and have sufficient concentrations of U and Pb for large signal intensities.

2. Sample Preparation

[5] All zircon samples were processed and separated using standard gravimetric and magnetic separation techniques at the University of Idaho. Zircon grains, both standards and unknowns, were mounted in a 1-inch diameter epoxy puck that was ground and polished to expose the grains. Photomicrograph maps and CL (cathodoluminescence) images were used to characterize the internal features of zircons such as growth zones and inclusions and to provide a base map for recording laser spot locations

3. Instrumentation

[6] All laser work in this study was performed using a New Wave UP-213 laser ablation system in conjunction with a ThermoFinnigan Element2 single collector double-focusing magnetic sector ICP-MS in the GeoAnalytical Lab at Washington State University. In comparison to a quadrupole ICP-MS, the Element2 has flat-top peaks and higher sensitivity, resulting in larger Pb signals, better counting statistics, and more precise and accurate measurement of isotope ratios. Fixed 30 or 40 μm diameter spots were used with a laser frequency of 10 Hz. The ablated material is delivered to the torch by He and Ar gas. Instrument details and operation parameters are listed in Table 1.

[7] For solution nebulization, the Element2 has a sensitivity of $\sim 2 \times 10^9$ cps (counts per second) per ppm for ^{238}U. At 40 μm beam size and $\sim$10 J/cm^2 laser fluency with the New Wave Nd:YAG 213 nm laser system, the signal intensity for ^{238}U is about 40,000 cps/ppm on NIST 612 glass which has a U concentration of 37 ppm.

4. Data Acquisition and Operational Parameters

[8] Each analysis consisted of a 6 second warm-up, an 8 second delay to enable the sample to reach the plasma, and 35 seconds of rapid scanning across masses ^{202}Hg, ^{204}(Hg + Pb), ^{206}Pb, ^{207}Pb, ^{208}Pb, ^{232}Th, ^{235}U, and ^{238}U. The Element2 was operated in the e-scan (electric scan) mode where the magnetic field strength is kept constant while the

Table 1. Instrument Details and Operation Parameters

	Description/Value
Laser Source	
Model	New Wave Research UP-213
Type	Nd:YAG
Wavelength	213 nm
Repetition rate	10 Hz
Energy density	~5.5–10.5 J/cm^2
Ablation strategy	spot, 30–40 μm
Warm-up	6–8 seconds
Delay	12–16 seconds
Dwell time	46 – 48 seconds
Focusing	on sample surface
ICP-MS	
Model	Element2, ThermoFinnigan
ICP torch	capacitive decoupling
RF Power	1250 W
Cooling gas	15 l/min
Auxiliary gas	0.9 l/min
Sample gas (Ar)	1.000 – 1.075 l/min
Carrier gas	He, ~1.3 l/min
Dead time	16 ns for counting mode
Scan mode	E-scan

accelerating voltage and the coupled ESA voltage is scanned allowing quick capture of the transient signals produced by the laser. One pre-scan was used to settle the magnet on the starting mass (202) before data acquisition begins. At low resolution, the Element2 produces a flat-top peak shape, with the peak flat comprising about 20% of the entire peak. We sampled the central 5% of the peak (3 points) in order to minimize the effects of minor peak drift. Each analysis consists of 300 sweeps, which takes about 35 seconds. Data acquisition parameters are summarized in Table 2.

[9] The Element2 has two detector modes: pulse counting and analog. Counting mode can be used for signals up to about 4×10^6 cps and analog mode is suitable for a range of 10^5–10^{10} cps. Counting mode is generally appropriate for measurement of ^{202}Hg, ^{204}(Pb + Hg), ^{206}Pb, ^{207}Pb, ^{208}Pb, and ^{235}U. Analog mode is used for ^{232}Th and ^{238}U when count rates exceed the upper limit of the counting mode. A gas blank was collected before each analysis with the plasma on but laser not firing. Blanks are collected with all masses in counting mode, as the noise of analog mode is high and will produce unrealistically high background signals.

[10] The Element2 was tuned before each analytical session using the NIST 612 glass standard to maximize signal intensity and stability. All operating parameters, including ICP-MS and laser settings, were held constant for standards and unknowns to minimize any potential bias between samples and standards. At the beginning of each analytical session, a zircon standard was analyzed until fractionation was stable and the variance in the measured ^{206}Pb/^{238}U and ^{207}Pb/^{206}Pb ratios was at or near 1% (1 sigma standard deviation). During a session the standard was analyzed two to three times every 5–10 unknown analyses.

5. Fractionation and Common Pb Correction in LA-ICP-MS Analysis

[11] Accurate correction for mass and elemental fractionation is one of the major challenges to achieving high levels of accuracy in LA-ICP-MS measurements [e.g., *Jackson*, 2001]. Total fractionation consists of static fractionation, where the measured ratio does not change with time, and time-dependent fractionation, where measured isotope ratios change during the course of the analysis. Static fractionation may be caused by space-charge effects [*Hieftje*, 1992; *Tanner et al.*, 1994], different ionization efficiencies for different elements [*Hirata and Nesbitt*, 1995], and non-stoichiometric evaporation and condensation due to the different volatility of elements [*Chan et al.*, 1992; *Jackson et al.*, 1992; *Outridge et al.*, 1997; *Eggins et al.*, 1998; *Jackson*, 2001]. In contrast, time-dependent fractionation is laser-induced. As the laser ablates the sample the depth/width aspect ratio of the pit gets larger and condensation on the pit wall will increase. This will favor release of more volatile elements, resulting in an increase of the ^{206}Pb/^{238}U and ^{207}Pb/^{235}U ratios over time [e.g., *Fryer et al.*, 1993, 1995; *Hirata and Nesbitt*, 1995; *Eggins et al.*, 1998; *Mank and Mason*, 1999; *Jackson*, 2001]. This time-dependent Pb/U fractionation is consistently observed during zircon spot analyses as seen in Figure 1.

Table 2. Acquisition Parameters

	Description/Value
Isotopes measured	^{202}Hg, ^{204}(Pb+Hg), ^{206}Pb, ^{207}Pb, ^{208}Pb, ^{232}Th, ^{235}U, ^{238}U
Settling time, ms	1
Samples per peak	60
Mass Window, %	5
Points per peak	3
Sample time, ms	4
Detector Mode	analog for ^{232}Th ^{238}U, counting for others
Total time per isotope, ms	13
Pre-scan	1
Total passes (sweeps)	300

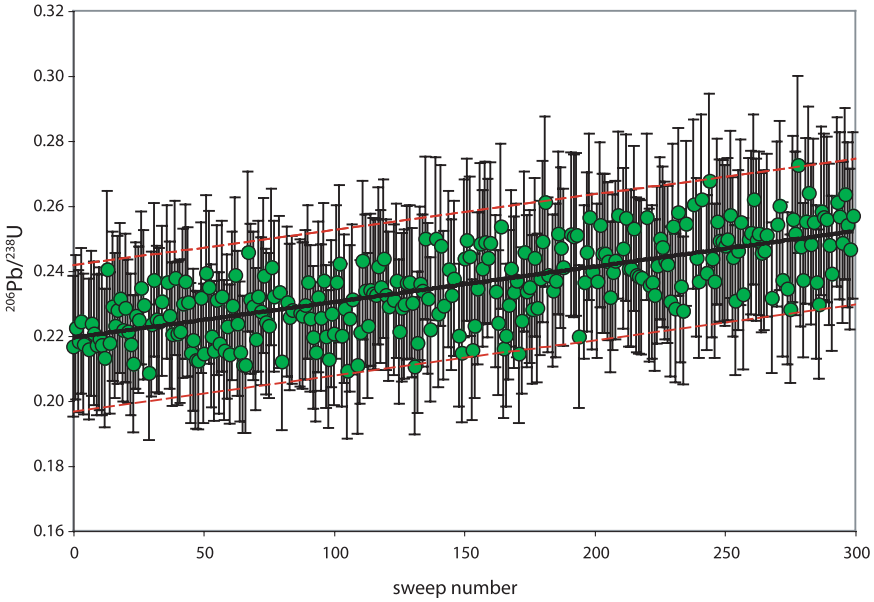

Figure 1. Time-dependent fractionation and correction with the mathematical intercept method. The solid line is the regression line calculated through all data points. The dashed lines show the 95% confidence range of the regression line. Data points beyond these two dashed lines have been filtered out. The error bars on each data point have been arbitrarily assigned at ± 10% to show the relative variation of individual ratios.

[12] Time-dependent fractionation was corrected using the intercept method, which assumes that the fractionation trend over the signal acquisition time is linear (e.g., see Figure 1) and the intercept at time 0 is assumed to be free of laser-induced time-dependent fractionation [*Sylvester and Ghaderi*, 1997]. Fractionation factors for correction of mass and elemental fractionation were determined by comparison of the $^{206}Pb/^{238}U$ intercept from standard analyses to the accepted $^{206}Pb/^{238}U$ value for that standard (determined by TIMS). The $^{207}Pb/^{206}Pb$ value is not measurably time-dependent over the duration of the analysis, and therefore the mean was used for determining the $^{207}Pb/^{206}Pb$ fractionation factor rather than intercept. The corresponding fractionation factors were then applied to the unknown zircons in order to calculate the fractionation corrected $^{206}Pb/^{238}U$ and $^{207}Pb/^{206}Pb$ ratios. Fractionation factors during this study ranged from 0.93 to 1.02 for $^{206}Pb/^{238}U$ and 0.99–1.01 for $^{207}Pb/^{206}Pb$. The implicit assumption in this approach is that differences in the zircon matrix will have an insignificant effect on the value of the fractionation factors, i.e., that fractionation effects will be the same in standards and unknowns, which is not strictly true in all cases [*Black*, 2005]. The reported $^{207}Pb/^{235}U$ values are derivative from the $^{206}Pb/^{238}U$ and $^{207}Pb/^{206}Pb$ ratios. The $^{207}Pb/^{235}U$ ratios and ages were also calculated directly from the measured ^{207}Pb and ^{235}U intensities as a check on the derivative $^{207}Pb/^{235}U$ calculations.

[13] Most LA-ICP-MS Pb isotopic measurements likely contain a small contribution from common Pb derived from various sources including the instrument, foreign material on the sample puck surface, and the zircon itself. Ideally, the common Pb component would be corrected by monitoring ^{204}Pb. However, the low intensity ^{204}Pb signal is masked by a significant isobaric interference with ^{204}Hg due to the presence of Hg at trace levels in our argon gas. Our approach was to measure the ^{202}Hg and ^{204}total (Pb + Hg) in the blank and then subtract both of these from the zircon analysis on a ratio-by-ratio basis. The abundance of ^{204}Hg is calculated from blank-corrected ^{202}Hg on the basis of the natural $^{202}Hg/^{204}Hg$ ratio, which in turn is subtracted from ^{204}total to yield ^{204}Pb. Using this approach our mean value for calculated ^{204}Pb was always approximately zero, but with exceptionally high variation (e.g., 5 ± 850 cps) which makes the value essentially unusable. Thus we were unable to reliably apply a correction for common lead using measured ^{204}Pb.

6. Data Reduction and Error Propagation

[14] Data reduction was performed off-line using an Excel program supplemented with Visual Basic

macros with the following steps: (1) Count rates for blanks were calculated by averaging the signal intensities of the 300 passes (sweeps), with spikes more than twice the average filtered out. The blank was then subtracted from the corresponding sample analysis. (2) The isotope ratios $^{206}Pb/^{238}U$ and $^{207}Pb/^{206}Pb$ were calculated for every sweep using the blank-corrected signal intensities. (3) The ratios of 300 sweeps were plotted on time series diagrams, a straight line fit through the data by least squares regression, and points outside of the 95% confidence range of the regression line removed by an Excel macro (Figure 1). (4) The intercept and standard error of the $^{206}Pb/^{238}U$ intercept were calculated using the Excel function Linest. For the $^{207}Pb/^{206}Pb$ ratio, the in-run error is simply the standard error as calculated on the mean of the $^{207}Pb/^{206}Pb$ measurements. (5) Fractionation factors were determined on the basis of the ratio of the "true" $^{206}Pb/^{238}U$, $^{207}Pb/^{235}U$, and $^{207}Pb/^{206}Pb$ values for the standard to their measured values (FF = true ratio/measured ratio). (6) These fractionation factors were applied to the unknowns in order to calculate the corrected ratios (corrected ratio = measured ratio × FF). Final ages and uncertainties were calculated using the corrected ratios and their associated uncertainties.

[15] The total error for each laser analysis is based on two sources: uncertainty in the determination of the intercept (in the case of $^{206}Pb/^{238}U$) or mean values (in the case of $^{207}Pb/^{206}Pb$) and uncertainty from the determination of the fractionation factors. In-run error estimates for intercept values of $^{206}Pb/^{238}U$ and mean values of $^{207}Pb/^{206}Pb$ average 2% and 1%, respectively, at the 2σ level. The fractionation factor error is based on the variance in the measurement of the standards calculated as 2 SD of the population. Uncertainty in the fractionation factors range from 1–3% for $^{206}Pb/^{238}U$ and 1–2% for $^{207}Pb/^{206}Pb$. The two sources of uncertainty are combined quadratically to determine an overall analysis error. However, propagation of the uncertainty in the fractionation correction varies with sample type. For samples in which each grain represents a stand-alone age determination, such as detrital samples where grains have no demonstrable genetic link to one another, errors are quadratically combined for each analysis. For samples in which grains are genetically related, such as zircons from igneous samples that record a single magmatic event, uncertainty in the fractionation correction is applied to the calculated weighted mean $^{206}Pb/^{238}U$ or $^{207}Pb/^{206}Pb$ age. The latter is the method employed in this study. Ages are calculated from $^{206}Pb/^{238}U$ or $^{207}Pb/^{206}Pb$ ratios for samples younger and older that 1.0 Ga, respectively. In cases where analyses were obtained during multiple analytical sessions, age determinations and associated uncertainties are calculated for each session to accommodate the variation in fractionation factor uncertainty between sessions.

[16] Our calculated errors do not take into account uncertainty in the TIMS values of the standard or any bias that might exist between the analysis of the standard and unknown zircon due to matrix or cumulative instrumental effects [*Black et al.*, 2004]. The uncertainties in the TIMS values of the standard are small (up to 0.7%, 2σ) relative to the other sources of error and have been neglected. The uncertainty due to any bias that might exist in the analysis of the standard and unknown zircon, however, is potentially significant. Analyses of currently used zircon standards indicate uncertainty due to matrix effects may be as large as 2% [*Black*, 2005]. Since there is currently no way to know, a priori, for any given unknown zircon, if any such bias exists, a minimum uncertainty of 2% should probably be assumed for all LA-ICP-MS age determinations.

7. Results

[17] Zircon ages were determined for five samples previously analyzed by TIMS and/or SHRIMP using our in-house standard, Peixe, to calculate fractionation factors. Ages of these samples range from circa 56 Ma to 1780 Ma. The results of our U-Pb analyses are listed in Table 3. A summary of the ages and how they compare with the TIMS ages determined for these samples is shown in Tables 4 and 5. All errors are reported at the 95% confidence level. The results also are shown on Tera-Wasserberg plots and weighted average plots using Isoplot [*Ludwig*, 2001]. Peixe is used as the zircon standard for calculation of all ages. Three samples (94–35, Temora, 91500) were analyzed using a 40 μm laser beam diameter and laser energy density of ~10 J/cm^2. For 2 samples (AS57, MCC12-515E), these parameters resulted in ^{206}Pb signals too large to be analyzed with the multiplier (counting mode). The laser beam diameter was reduced to 30 μm to compensate for this. Analyses of the Peixe standard corresponding to these samples were performed

Table 3 (Representative Sample). LA-ICP-MS Data and Calculated Ages[a] [The full Table 3 is available in the HTML version of this article at http://www.g-cubed.org]

		Ratios						Ages					
Spot	Session	$^{206}Pb/^{238}U$	±2 σ	$^{207}Pb/^{235}U$	±2 σ	$^{207}Pb/^{206}Pb$	±2 σ	$^{206}Pb/^{238}U$	±2 σ	$^{207}Pb/^{235}U$	±2 σ	$^{207}Pb/^{206}Pb$	±2 σ
						Zircon 94-35							
9435_1A	1	0.00903	0.00021	0.05991	0.00203	0.04811	0.00221	58.0	1.3	59.1	1.9	104	111
9435_2A	1	0.00901	0.00023	0.06014	0.00215	0.04843	0.00207	57.8	1.5	59.3	2.1	120	102
9435_2B	1	0.00881	0.00017	0.05817	0.00185	0.04789	0.00172	56.5	1.1	57.4	1.8	94	86
9435_2C	1	0.00899	0.00020	0.05577	0.00187	0.04498	0.00230	57.7	1.3	55.1	1.8	0	9
9435_3A	1	0.00880	0.00021	0.05930	0.00204	0.04887	0.00224	56.5	1.3	58.5	2.0	141	110
9435_3B	1	0.00882	0.00021	0.06095	0.00211	0.05010	0.00248	56.6	1.4	60.1	2.0	199	117
9435_10B	2	0.00857	0.00024	0.06133	0.00424	0.05194	0.00309	55.0	1.6	60.4	4.1	283	139
9435_10E	2	0.00860	0.00024	0.05390	0.00315	0.04545	0.00212	55.2	1.6	53.3	3.0	0	48
9435_10F	2	0.00869	0.00022	0.05427	0.00347	0.04530	0.00248	55.8	1.4	53.7	3.3	0	51
9435_10V	2	0.00858	0.00026	0.05413	0.00392	0.04578	0.00286	55.1	1.6	53.5	3.8	0	119
9435_9A	2	0.00858	0.00022	0.05755	0.00296	0.04867	0.00193	55.1	1.4	56.8	2.8	132	95
9435_9B	2	0.00867	0.00023	0.05721	0.00354	0.04786	0.00248	55.6	1.5	56.5	3.4	93	125
9435_9C	2	0.00869	0.00021	0.05772	0.00308	0.04819	0.00207	55.8	1.3	57.0	3.0	108	103
9435_9D	2	0.00875	0.00020	0.06375	0.00318	0.05282	0.00208	56.2	1.3	62.8	3.0	321	91
9435_9G	2	0.00870	0.00021	0.05680	0.00286	0.04737	0.00185	55.8	1.3	56.1	2.7	68	94
9435_9H	2	0.00884	0.00024	0.05811	0.00355	0.04770	0.00241	56.7	1.5	57.4	3.4	85	122
9435_9I	2	0.00858	0.00022	0.05761	0.00340	0.04871	0.00238	55.1	1.4	56.9	3.3	134	117
9435_9J	2	0.00884	0.00022	0.05901	0.00338	0.04842	0.00230	56.7	1.4	58.2	3.2	120	114
9435_9K	2	0.00858	0.00023	0.06251	0.00364	0.05287	0.00252	55.1	1.4	61.6	3.5	323	110
9435_9O	2	0.00879	0.00018	0.05940	0.00319	0.04900	0.00221	56.4	1.2	58.6	3.1	148	107
9435_9Q	2	0.00884	0.00023	0.05982	0.00346	0.04910	0.00231	56.7	1.5	59.0	3.3	152	112
9435_9R	2	0.00850	0.00023	0.05913	0.00342	0.05048	0.00237	54.5	1.5	58.3	3.3	217	111
9435_9S	2	0.00856	0.00021	0.05737	0.00322	0.04859	0.00222	55.0	1.4	56.6	3.1	128	109
						Zircon Temora							
Temora_10A	1	0.06733	0.00096	0.50984	0.01466	0.05492	0.00049	420	6	418	10	409	20
Temora_11A	1	0.06550	0.00138	0.49383	0.01616	0.05468	0.00061	409	8	408	11	399	25
Temora_12B	1	0.06648	0.00233	0.50973	0.02201	0.05562	0.00088	415	14	418	15	437	35
Temora_13A	1	0.06611	0.00185	0.50441	0.01897	0.05534	0.00073	413	11	415	13	426	30
Temora_13B	1	0.06717	0.00202	0.51568	0.02022	0.05569	0.00074	419	12	422	13	440	30
Temora_10A	1	0.06733	0.00096	0.50984	0.01466	0.05492	0.00049	420	6	418	10	409	20
Temora_2G	1	0.06671	0.00082	0.51304	0.01707	0.05578	0.00115	416	5	420	11	444	46
Temora_4A	1	0.06686	0.00100	0.50112	0.01847	0.05437	0.00106	417	6	412	12	386	44
Temora_5A	1	0.06674	0.00233	0.51065	0.02811	0.05549	0.00128	416	14	419	19	432	52
Temora_6A	1	0.06622	0.00241	0.51152	0.02968	0.05602	0.00151	413	15	419	20	453	61
Temora_6B	1	0.06575	0.00226	0.49764	0.02717	0.05489	0.00125	411	14	410	18	408	51
Temora_6C	1	0.06697	0.00122	0.50987	0.01574	0.05522	0.00055	418	7	418	11	421	22

[a] Fractionation factor uncertainty is not incorporated into the reported uncertainties. Please see text for explanation.

Table 4. Comparison of Age Determinations During Different Analytical Sessions[a]

	Without FF Error	With FF Error
94–35[b]		
Session 1	57.1 ± 0.5	57.1 ± 1.4
Session 2	55.7 ± 0.3	55.7 ± 1.0
Average	**56.4 ± 0.4**	**56.4 ± 1.2**
Temora[b]		
Session 1	418 ± 2	418 ± 10
Session 2	417 ± 1	417 ± 8
Session 3	420 ± 1	420 ± 13
Session 4	410 ± 1	410 ± 11
Session 5	412 ± 2	412 ± 7
Session 6	418 ± 1	418 ± 7
Average	**416 ± 1**	**416 ± 9**
91500[c]		
Session 1	1055 ± 6	1055 ± 17
Session 2	1055 ± 4	1055 ± 20
Average	**1055 ± 5**	**1055 ± 18**

[a] Fractionation factor uncertainties are added quadratically to the uncertainties of the weighted means of corresponding sessions. Uncertainties reported at 95% confidence level.
[b] Ages determined from $^{206}Pb/^{238}U$ ratios.
[c] Ages determined from $^{207}Pb/^{206}Pb$ ratios.

with the same parameters to allow for a consistent determination of fractionation factors.

7.1. Peixe

[18] The zircon standard Peixe was provided by George Gehrels of the University of Arizona, where it has been in use as an in-house zircon standard [*Dickinson and Gehrels*, 2003]. This sample is from the Rio de Peixe area of Brazil. Zircons from Peixe are typically large, ranging up to 1 cm in diameter, clear, colorless, inclusion free, and sector zoned in CL. An ID-TIMS age of 564 ± 4 Ma for Peixe is based on 4 concordant analyses (G. Gehrels, unpublished data).

7.2. 94–35

[19] Zircon sample 94–35, from an undeformed tonalite pluton of the Coast Mountains batholith, Alaska, has a reported TIMS age of 55.5 ± 1.5 Ma based on five fractions [*Klepeis et al.*, 1998]. Twenty-three LA-ICP-MS analyses on 5 grains collected in two analytical sessions yield a weighted mean $^{206}Pb/^{238}U$ age of 56.1 ± 0.4 Ma (MSWD = 2.0) (Figure 2). Age determinations for each session, incorporating the uncertainty in the fractionation correction after calculation of the weighted mean, are 57.1 ± 1.4 and 55.7 ± 1.0 Ma. Combining these results yields an assigned unweighted average age of 56.4 ± 1.2 Ma (Table 4). The relatively large uncertainty in the $^{207}Pb/^{206}Pb$ ratios (up to 6%; Table 3) reflects difficulty in measuring ^{207}Pb in young samples. Nevertheless, most analyses are concordant (Figure 2). The discordance observed for some fractions is interpreted to reflect incorporation of slight components of common Pb.

7.3. Temora

[20] Zircon sample Temora is from the Middledale Gabbroic Diorite, New South Wales, Australia, and has been proposed as a zircon standard by *Black et al.* [2003], who reported a weighted average $^{206}Pb/^{238}U$ age of 416.8 ± 1.1 Ma based on 21 ID-TIMS analyses and 416.8 ± 1.8 Ma based on 50 SHRIMP analyses. Ninety-three spot LA-ICP-MS analyses on 21 grains of Temora were collected in 6 separate sessions spanning 3 months. All analyses, corrected for fractionation but not incorporating fractionation factor uncertainty, give a weighted mean $^{206}Pb/^{238}U$ age of 415 ± 1 Ma (MSWD = 2.5, Figure 3), which is within error of the ID-TIMS age. The relatively high MSWD is interpreted to reflect variation in the fractionation factor, which is not represented in the uncertainty

Table 5. Summary of LA-ICPMS Ages and Comparison With TIMS Ages[a]

Sample	n	TIMS Age, Ma	Age Without FF Uncertainty	Age With FF Uncertainty	Age Range	Maximum Difference[b]	Age Ref.[c]
94–35	23	55.5 ± 1.5	56.4 ± 0.4	56.4 ± 1.2	54.5–58.0	4.5%	1
Temora	93	416.8 ± 1.1	416 ± 1	416 ± 9	403–429	3.4%	2
91500	29	1065.4 ± 0.3	1055 ± 5	1055 ± 18	1036–1080	2.7%	3
AS57	14	1099.1 ± 1.2	1099 ± 3	1099 ± 40	1089–1107	0.9%	4
MCC12-515E	11	~1778	1779 ± 4	1779 ± 33	1770–1790	0.7%	5

[a] Uncertainties reported at 95% confidence level. Ages for 94–35 and Temora are determined from $^{206}Pb/^{238}U$ ratios; ages for 91500, AS57, and MCC12-515E are determined from $^{207}Pb/^{206}Pb$ ratios.
[b] This value reports maximum difference between individual LA-ICPMS spot analyses and the TIMS age.
[c] Age references: 1, *Klepeis et al.* [1998]; 2, *Black et al.* [2003]; 3, *Wiedenbeck et al.* [1995]; 4, *Paces and Miller* [1993] and *Schmitz et al.* [2003]; 5, *Premo* [1991].

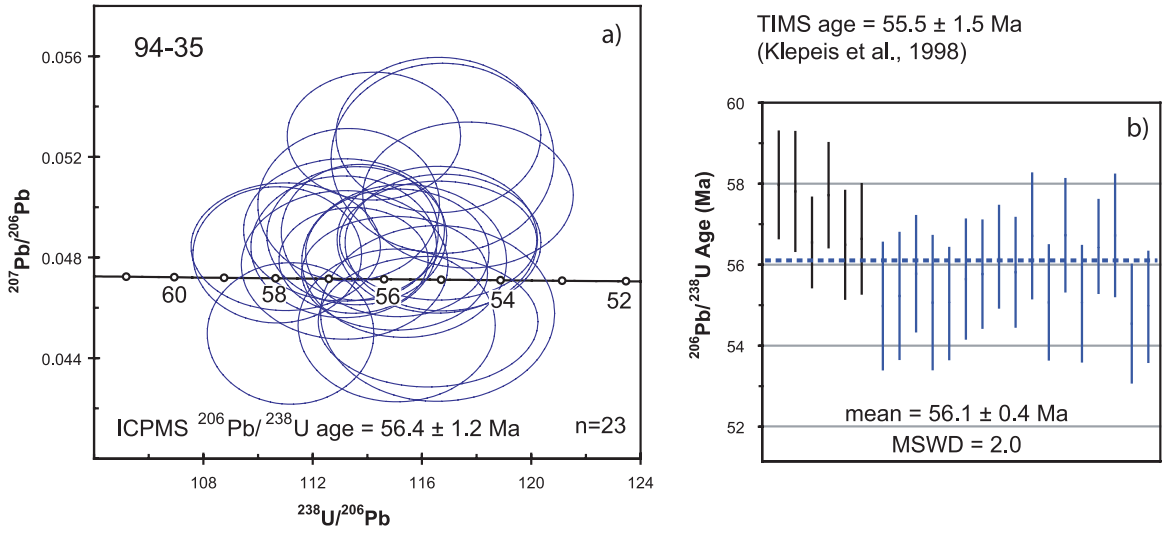

Figure 2. LA-ICP-MS data of zircon 94–35 plotted on (a) Tera-Wasserburg and (b) $^{206}Pb/^{238}U$ weighted mean plots. See text for discussion of age determinations and reported uncertainties.

above. Ages determined by quadratically adding the fractionation uncertainty after calculating weighted mean ages for each analytical session (Table 4) vary from 410 ± 11 to 420 ± 13 Ma. An unweighted average of these sessions results in a mean age of 416 ± 9 Ma.

7.4. 91500

[21] Our sample of 91500 is a single zircon crystal from a pegmatite in Ontario, Canada, and has been widely used as a zircon standard due to its large size and previous availability. *Wiedenbeck et al.* [1995] reported $^{206}Pb/^{238}U$ and $^{207}Pb/^{206}Pb$ ages of 1062.4 ± 0.4 and 1065.4 ± 0.3 Ma, with a significant degree of discordance. Twenty-nine spot analyses of 5 fragments collected in two analytical sessions yield a weighted mean $^{207}Pb/^{206}Pb$ age of 1055 ± 4 Ma (MSWD = 1.2; Figure 4). Incorporating the uncertainty in fractionation, ages for each session are 1055 ± 17 and 1055 ± 20 Ma. An unweighted average of these sessions results in an age of 1055 ± 18 Ma.

7.5. AS57

[22] Zircon sample AS57 is from the anorthositic series of the Duluth Complex and has been described and dated by *Paces and Miller* [1993]

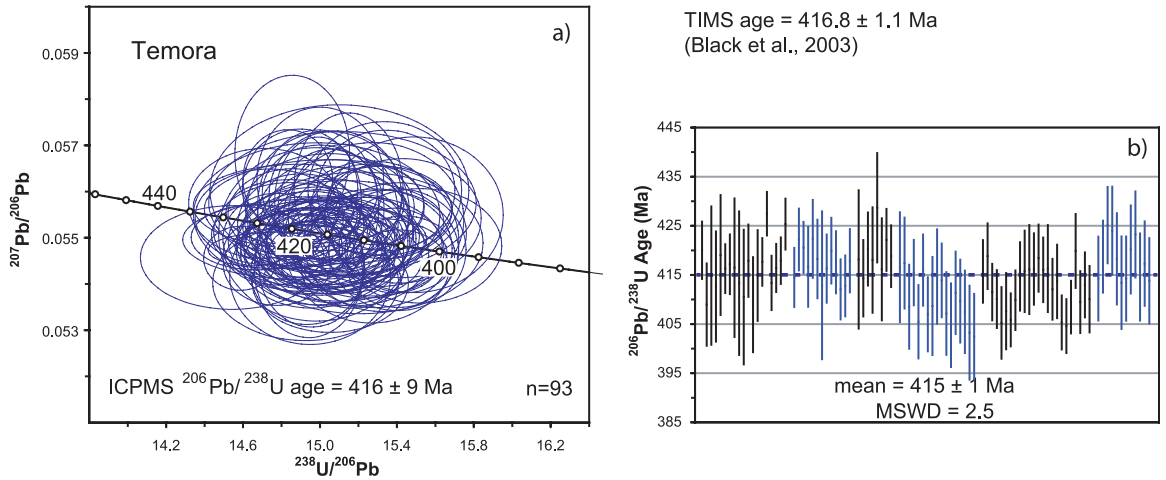

Figure 3. LA-ICP-MS data of zircon Temora plotted on (a) Tera-Wasserburg and (b) $^{206}Pb/^{238}U$ weighted mean plots. See text for discussion of age determinations and reported uncertainties.

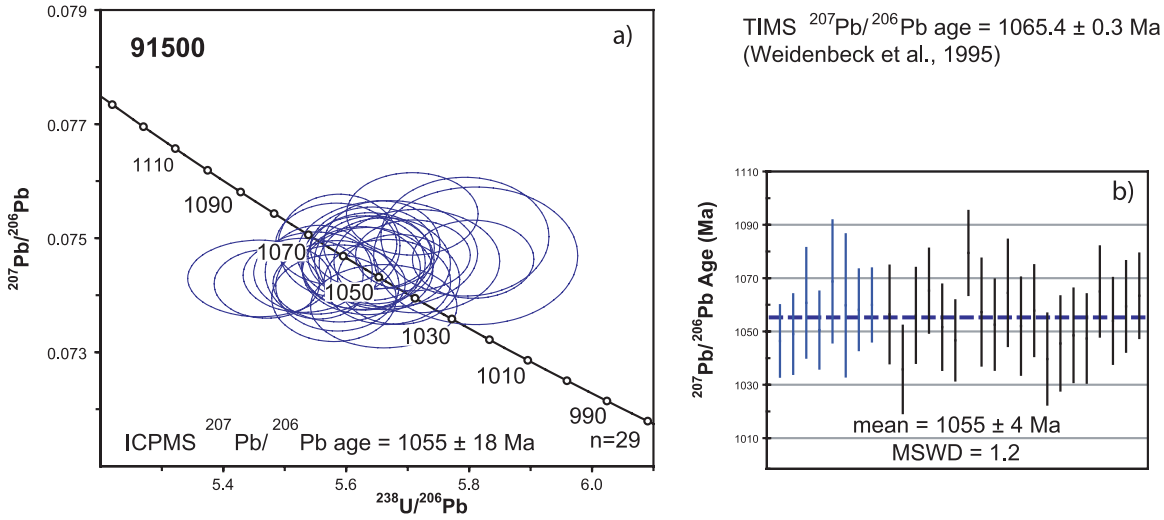

Figure 4. LA-ICP-MS data of zircon 91500 plotted on (a) Tera-Wasserburg and (b) $^{207}Pb/^{206}Pb$ weighted mean plots. See text for discussion of age determinations and reported uncertainties.

and *Schmitz et al.* [2003]. The concordia age is 1099.1 ± 1.2 Ma, with minor discordance up to a maximum of 2%. Fourteen spot analyses of a single crystal of AS57 yield a weighted mean $^{207}Pb/^{206}Pb$ age of 1099 ± 3 Ma (MSWD = 1.2; Figure 5), within error of the ID-TIMS age. A large uncertainty (2%, 2σ SD) in the $^{207}Pb/^{206}Pb$ value of the Peixe standard for this analytical session results in an assigned age with a high error of 1099 ± 40 Ma.

7.6. MCC12-515E

[23] Zircon sample MCC2-515E is from the Mullen Creek Complex of the Green Mountain Formation, northwest Colorado, a juvenile Proterozoic granitoid dated at approximately 1778 Ma [*Premo*, 1991]. Eleven spot analyses were made on 4 grains of MCC12-515E. The weighted mean $^{207}Pb/^{206}Pb$ age is 1779 ± 4 Ma (MSWD = 1.7; Figure 6). With incorporation of the fractionation uncertainty, the age is 1779 ± 33 Ma. As for AS57 above, the higher uncertainty is due to the large uncertainty in

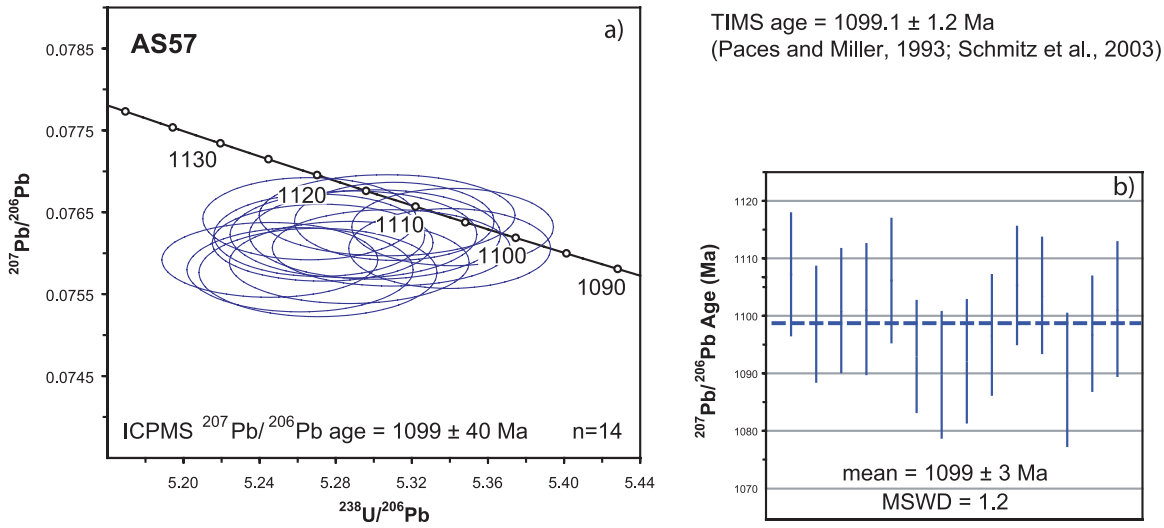

Figure 5. LA-ICP-MS data of zircon AS57 plotted on (a) Tera-Wasserburg and (b) $^{207}Pb/^{206}Pb$ weighted mean plots. The age determination in Figure 5a includes fractionation uncertainty quadratically added to the weighted mean reported in Figure 5b.

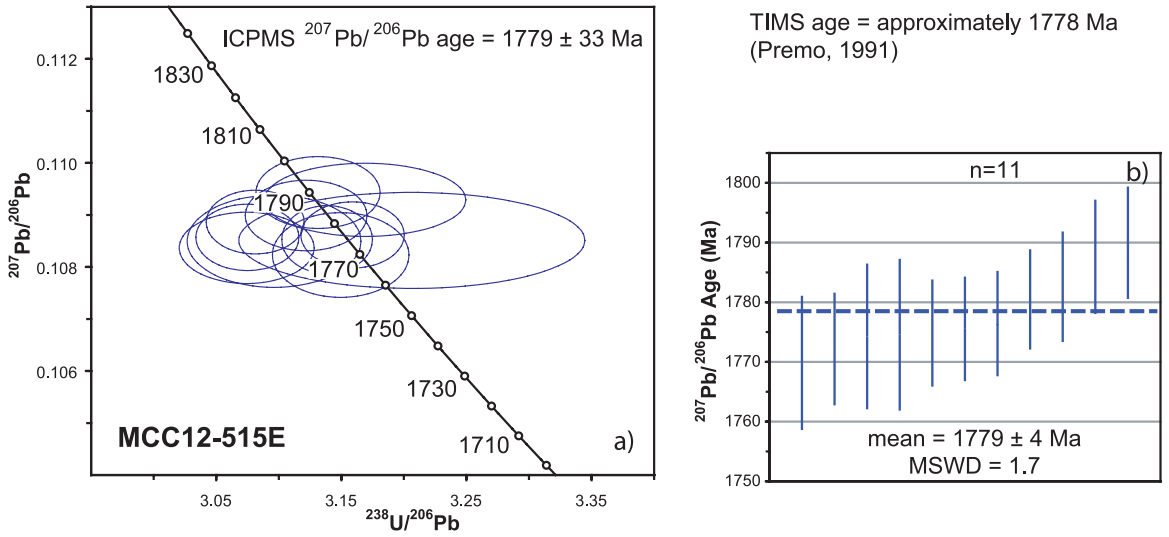

Figure 6. LA-ICP-MS data of zircon MCC12-515E plotted on (a) Tera-Wasserburg and (b) $^{207}Pb/^{206}Pb$ weighted mean plots. The age determination in Figure 6a includes fractionation uncertainty quadratically added to the weighted mean reported in Figure 6b.

the $^{207}Pb/^{206}Pb$ fractionation factor from Peixe for that session (1.9%, 2σ SD).

8. Discussion and Conclusions

8.1. Accuracy and Precision

[24] The ages determined by LA-ICP-MS for the five zircon samples in this study agree well with the previously published TIMS ages. As expected, the precision and accuracy of the $^{206}Pb/^{238}U$ and $^{207}Pb/^{206}Pb$ ages vary with the age and character of the different samples. The $^{206}Pb/^{238}U$ ages for 94–35 (56.4 ± 1.2 Ma) and Temora (416 ± 9 Ma) are consistent with the available TIMS ages of 55.5 ± 1.5 Ma [*Klepeis et al.*, 1998] and 416.8 ± 1.1 Ma [*Black et al.*, 2003], respectively.

[25] The data for the Paleozoic sample Temora illustrates the potential reproducibility, precision, and accuracy of the LA-ICP-MS method. Shown in Figure 3 are 93 analyses of Temora. These data were collected on 6 different days, over a period of more than 2 months, and represent the application of 6 independently determined fractionation factors. In spite of these different operating conditions the largest deviation in $^{206}Pb/^{238}U$ age using individual LA-ICP-MS spot analyses from the TIMS value among the six sessions was 3.4%; the total range of age determinations was 429 to 403 Ma for all 93 analyses. Variation in $^{206}Pb/^{238}U$ determinations for the younger 94–35 was only slightly greater with the largest deviation from the TIMS value being 4.5% and the total range of ages 58.0 to 54.5 Ma for 23 analyses. The maximum ~4% deviation of $^{206}Pb/^{238}U$ ages from the TIMS age for individual spot analyses provides an approximation of the expected uncertainty of individual analyses for applications such as detrital studies.

[26] The remaining 3 Proterozoic samples analyzed also yielded $^{207}Pb/^{206}Pb$ ages within uncertainty of the TIMS values. Sample 91500 had the largest difference (0.9%) between the weighted mean LA-ICP-MS and the TIMS ages. The lower LA-ICP-MS age could be due to discordance that is known to exist in 91500 [*Wiedenbeck et al.*, 1995]. The $^{207}Pb/^{206}Pb$ ages of individual spot analyses have a maximum deviation from the TIMS age of 2.7% (Table 5), which may be due in part to sample heterogeneity or the presence of common Pb.

[27] The Mesoproterozoic sample AS57 is only slightly older than 91500, but its U and Pb concentrations are much higher. The ^{206}Pb signal intensity for this sample exceeds the upper limit of the counting mode of the detector using the standard instrument parameters for the other samples. The counting mode is preferred for the external standard Peixe, however, because it does not have enough ^{206}Pb to be measured with any accuracy in the analog mode, even with very high laser energy intensity and large beam size (40 μm). To accommodate the high ^{206}Pb in AS57, the sample and Peixe were analyzed with a smaller beam size (30 μm) and laser energy

intensity (~5.5 J/cm^2). The resulting age determinations for AS57 were in good agreement with the TIMS age of 1099.1 Ma [*Paces and Miller*, 1993]. The $^{207}Pb/^{206}Pb$ ages of individual spot analyses have a maximum deviation of 1.1% from the TIMS age. However, the smaller beam size and lower energy intensity result in very low ^{207}Pb count rates of Peixe, leading to much higher errors in determination of the fractionation factors. If this uncertainty is propagated into the final in-run uncertainty for individual analyses, the precision of the $^{207}Pb/^{206}Pb$ spot analyses would be ~4% which is poorer than observed for the other Proterozoic samples. This is a problem with matching of standards to unknown samples and is discussed further below.

8.2. Error Assignment

[28] In evaluating the final errors for the ages we report here, we have considered two main sources of error in the age determinations: uncertainties in the intercept of the unknown analyses, which are applied to the individual analyses, and uncertainties in the fractionation factors, which are applied after calculation of the weighted mean age. Both sources of uncertainty are incorporated into the individual analysis in detrital studies where each age determination is a stand-alone result. However, for igneous samples, the uncertainty of the weighted mean age should not be lower than the uncertainty due to the fractionation factors used to calculate the ages. If the fractionation factor uncertainty is incorporated before the weighted average ages are calculated, the resulting uncertainties can be unrealistically low, especially if the number of analyses (n) is large. This is demonstrated by our analysis of Temora. Incorporation of the fractionation factor uncertainty before a weighted mean is calculated results in a $^{206}Pb/^{238}U$ age of 414.6 ± 1.2 Ma. While this is within error of the TIMS age of 416.8 ± 1.1 Ma, it is not realistic given that the uncertainties in the $^{206}Pb/^{238}U$ fractionation factors for the individual sessions vary from 1.8 to 3.4% (2 SD).

[29] In order to quantify the uncertainty of the fractionation factor, we use the standard deviation of the standard analyses rather than the standard error of the population. For stand-alone analyses, this is appropriate because any single analysis could have the same variance as the measurements of the standards that bracket it. In the case of multiple analyses of a homogenous population, however, it is less clear that this is the appropriate method. For a group of analyses, especially when n is large, multiple analyses of an unknown will be likely to have approximately the same distribution as the analyses of the standard. Standard error is the measure of how well the fractionation factor has been determined from the group of standard analyses. Complications arise, however, in choosing n. If standard analyses are stable on a long time frame and all are included in the calculation of fractionation factors, then n will be large and the resulting standard error will be unrealistically small. On the other hand, use of standard analyses that immediately bracket the unknown analyses (i.e., sliding window) might be more realistic in terms of error assessment but a longer-term average may more accurately define the fractionation factors. Calculating uncertainty on the basis of the standards that immediately bracket the unknowns could be justified if all of the measured variation is due to changing machine conditions (i.e., instrumental drift), but is not justified when measured variations are due to sample heterogeneity which we know contribute to at least some of the variability in the standards.

[30] Analysis of the Paleoproterozoic sample MCC12-515E dramatically illustrates the complexity of error assignment for the LA-ICP-MS data. The Pb concentration for this sample is higher than AS57 and as a result, precision and accuracy, for both individual spot analyses and age determination, are better (Tables 4 and 5). The LA-ICP-MS weighted mean $^{207}Pb/^{206}Pb$ age for this sample is 1779 ± 4 Ma (MSWD = 1.7; Figure 6) using only the uncertainty in the intercept prior to calculation of the weighted mean age. However, incorporation of the uncertainty in the fractionation correction into the error quadratically *after* the calculation of the weighted mean, results in an imprecise age assignment of 1779 ± 33 Ma. In contrast to this imprecise age assignment is the narrow range of $^{207}Pb/^{206}Pb$ ages (1770 to 1790 Ma) for the 11 individual spot analyses with a maximum deviation of 0.7% from the TIMS age. The large error is due to the high variance (1.85%, 2 SD) in the measurement of $^{207}Pb/^{206}Pb$ in the Pb-poor Peixe. Both age determinations agree with the TIMS age of approximately 1778 Ma [*Premo*, 1991], but the errors, and their implications, are obviously much different.

8.3. Limitations and Considerations

[31] This study demonstrates the potential as well as the limitations of LA-ICP-MS U-Pb zircon

analysis. Some of the limitations of this method include (1) the lack of ideal standards to use to correct for instrumental mass and elemental bias; (2) the uncertainty in the behavior of different zircons (matrix effects); (3) the challenge of making common Pb corrections with many ICP-MS instruments; (4) the problems presented by U/Pb heterogeneity in zircon grains; and (5) the difficulty in measuring young, low U zircons.

[32] One of the major limitations of this technique is presented by the lack of an ideal set of standards. An ideal standard zircon would be concordant and have sufficient Pb for accurate and reproducible measurement of isotopic ratios. For many zircons, the irony is that if zircons have sufficient U to produce abundant Pb they often will have significant radiation damage that leads to Pb loss and U/Pb discordance. Conversely, lower U zircons are not as susceptible to Pb loss but typically have insufficient Pb, and particularly ^{207}Pb in younger zircons, for accurate analysis. A case in point is the use of Peixe for determining ^{207}Pb/^{206}Pb fractionation factors as discussed above.

[33] One promising solution to the standard dilemma may be to use the chemical abrasion technique of treating zircons to remove radiation damage zones in the crystal lattice [*Mattinson*, 2005]. *Mattinson* [2005] has demonstrated that removing these zones by partial dissolution treatment leads to greatly improved concordancy of the grains with only small removal of zircon volume. Chemical abrasion of zircon standards could potentially help address the dilemma of Pb loss that occurs to some extent in all of the zircon standards and would help improve the precision and accuracy in the determination of fractionation factors in LA-ICP-MS techniques that rely on external standards.

[34] Another limitation in the LA-ICP-MS U-Pb zircon technique is the potential for complex matrix affects that may result in different U/Pb fractionations in different zircons [*Black*, 2005]. The uncertainty that this produces (~2% based on *Black* [2005] and our unpublished data) is something that is currently not incorporated into the final errors for the individual spot analyses or final age assignments. The contribution of matrix effects to the uncertainty in accuracy of zircon analysis will need to be tested with more extensive examination of well-dated zircons.

[35] Inability to make an accurate common Pb correction is another unresolved problem in our LA-ICP-MS technique. The empirical evidence from this study suggests that common Pb does not appear to be a major factor within the precision of our analyses. Inclusion of significant amounts of common Pb in young samples can be detected by discordance of individual analyses along a discordia line extending toward the common Pb composition. If this spread is observed, as may be the case for sample 94–35, the analyses can be corrected by assuming concordance and applying a common Pb correction using the ^{207}Pb method [*Williams*, 1998]. For detrital samples with young zircons, common Pb-rich analyses will likely be rejected due to discordance. Older samples where the ^{207}Pb/^{206}Pb age is used are more problematic. The ^{207}Pb method for common Pb correction cannot be used since ^{207}Pb/^{206}Pb is the ratio of interest. However the presence of common Pb will likely cause scatter in the observed ^{207}Pb/^{206}Pb ages since common Pb is generally not uniformly distributed throughout a zircon population. For AS57, analyses with measured ^{206}Pb/^{204}Pb ratios of greater than 15,000 would yield ^{207}Pb/^{206}Pb ratios indistinguishable from the current data set. Analyses with measured ^{206}Pb/^{204}Pb ratios of less than 10,000 would result in ratios that lie outside the error of the fractionation correction uncertainty and thus be detectable by increased scatter. Assuming variable contributions of common Pb, samples with high variance in observed ^{207}Pb/^{206}Pb ratios can be interpreted to have high common Pb components and would thus be suspect.

[36] On the basis of the zircon data presented here, the LA-ICP-MS technique has the precision, and potentially the accuracy, of individual spot analyses that approach that of ion probe or SHRIMP analyses. The major difference between the two methods, however, is the volume of material ablated during the analysis. A 35-second laser analysis creates pits approximately 25 μm deep compared to a 2.5-μm pit in a typical SHRIMP analysis. In a homogenous zircon with simple systematics, this decreased spatial resolution does not present a problem for LA-ICP-MS analytical uncertainty. However, in complex zircons different domains representing xenocrystic cores, metamict zones, or overgrowths, may be sampled during the analysis. This is usually manifest in several ways. In the case of inherited cores or younger overgrowths, a change in ages is easily seen with increasing depth. In this scenario, age estimates for the different domains can potentially be deconvolved, but will lack precision.

[37] Finally, there is the problem of determining ages in young zircons, particularly those with low U concentrations. Of course this is not a problem unique to the LA-ICP-MS method, but is more acute due to the brevity of the analysis and the limitations imposed by counting statistics. For example, the measured ^{207}Pb counts for sample 94–35 are barely above the background counts, which result in large variations in the $^{207}Pb/^{206}Pb$ ratio and high uncertainties in calculated $^{207}Pb/^{206}Pb$ ages. For samples such as sample 94–35, in which analyses are concordant even with $^{207}Pb/^{206}Pb$ ratios of poor precision, we argue that assuming concordance and minimal common Pb, the calculated weighted mean $^{206}Pb/^{238}U$ age provides a reliable age estimate. Potential approaches to improving the analysis of young zircons need to rely on increasing the signal/noise ratio for ^{206}Pb and ^{207}Pb. Increasing the laser pit size or increasing laser energy intensity may also improve the quality of the analysis. Both methods however, increase the amount of zircon ablated and thereby increase the potential problems associated with measuring heterogeneous zircon zones as discussed above.

8.4. Summary

[38] In general, laser ablation U-Pb analysis of zircons using a high resolution ICP-MS such as the Element2 can be applied to samples with nearly full range of geological ages with a reasonable level of accuracy and precision. The relatively simple sample preparation and operation combined with short analytical time make it an ideal tool for detrital zircon studies. This technique is also suitable for reconnaissance age investigations. There are many applications where the precision and accuracy of the LA-ICP-MS technique is sufficient for answering a wide range of geological questions. Where more precise and accurate age information is required, it can provide important groundwork for more detailed analysis using the established TIMS and SHRIMP methods.

Acknowledgments

[39] Funding for this work has come, in part, from NSF grants OCE-0137365 and EAR-0230145 to Vervoort and from start-up funds provided by Washington State University, and from NSF grants EAR-0126299 and EAR-0208162 to McClelland. The authors would like to thank George Gehrels, who was instrumental in helping us develop the laser ablation ICP-MS technique at WSU by providing standards and offering frequent guidance. Constructive reviews by George Gehrels and Mary Reid greatly improved this manuscript. The authors would also like to thank Scott Cornelius for technical assistance related to sample preparation and imaging, Lance Black and Wayne Premo for providing the samples Temora and MCC12-515E, respectively, and Ken Ludwig for help with statistical questions.

References

Black, L. P. (2005), The use of multiple reference samples for the monitoring of ion microprobe performance during zircon $^{207}Pb/^{206}Pb$ age determinations, *Geostand. Newsl.*, *29*, 169–182.

Black, L. P., S. L. Kamo, C. M. Allen, J. N. Aleinikoff, D. W. Davis, R. J. Korsch, and C. Foudoulis (2003), TEMORA 1: A new zircon standard for Phanerozoic U-Pb geochronology, *Chem. Geol.*, *200*, 155–170.

Black, L. P., et al. (2004), Improved $^{206}Pb/^{238}U$ microprobe geochronology by the monitoring of a trace-element-related matrix effect: SHRIMP, ID–TIMS, ELA–ICP–MS and oxygen isotope documentation for a series of zircon standards, *Chem. Geol.*, *205*, 115–140.

Chan, W.-T., X. L. Mao, and R. E. Russo (1992), Differential vaporization during laser ablation/deposition of Bi-Sr-Ca-Cu-O superconducting materials, *Appl. Spectrosc.*, *46*, 1025–1031.

Dickinson, W., and G. Gehrels (2003), U-Pb ages of detrital zircons from Permian and Jurassic eolian sandstones of the Colorado Plateau, USA: Paleogeographic implications, *Sediment. Geol.*, *163*, 29–66.

Eggins, S. M., L. P. J. Kinsley, and J. M. M. Shelley (1998), Deposition and elemental fractionation processes during atmospheric pressure laser sampling for analysis by ICPMS, *Appl. Surf. Sci.*, *127–129*, 278–286.

Feng, R., N. Machado, and J. Ludden (1993), Lead geochronology of zircon by LaserProbe-Inductively Coupled Plasma Mass Spectrometry (LP-ICPMS), *Geochim. Cosmochim. Acta*, *57*, 3479–3486.

Fryer, B. J., S. E. Jackson, and H. Longerich (1993), The application of laser ablation microprobe-inductively coupled plasma-mass spectrometry (LAM-ICP-MS) to in situ (U)-Pb geochronology, *Chem. Geol.*, *109*, 1–8.

Fryer, B. J., S. E. Jackson, and H. P. Longerich (1995), The design, operation and role of the laser ablation microprobe coupled with an inductively coupled plasma-mass spectrometer (LAM-ICP-MS) in the Earth sciences, *Can. Mineral.*, *33*, 303–312.

Hieftje, G. M. (1992), Plasma diagnostic techniques for understanding and control, *Spectrochim. Acta*, *47B*, 3–25.

Hirata, T., and R. Nesbitt (1995), U-Pb isotope geochronology of zircon: Evaluation of the laser probe-inductively coupled plasma mass spectrometry technique, *Geochim. Cosmochim. Acta*, *59*, 2491–2510.

Horn, I., R. L. Rudnick, and W. F. McDonough (2000), Precise elemental and isotope ratio determination by simultaneous solution nebulization and laser ablation-ICP-MS: Application to U-Pb geochronology, *Chem. Geol.*, *164*, 281–301.

Jackson, S. E. (2001), The application of Nd:YAG lasers in LA-ICP-MS, in *Laser-Ablation-ICPMS in the Earth Sciences: Principles and Applications*, *Short Course Ser.*, vol. 20, edited by P. Sylvester, pp. 29–47, Mineral. Assoc. of Can., St. John's, Newfoundland, Canada.

Jackson, S. E., H. P. Longerich, G. R. Dunning, and B. J. Fryer (1992), The application of laser ablation microprobe-inductively coupled plasma-mass spectrometry (LAM-ICP-

MS) to in situ trace element determination in minerals, *Can. Mineral.*, *30*, 1049–1064.

Jeffries, T. E., J. Fernandez-Suarez, F. Corfu, and G. Gutierrez (2003), Advances in U-Pb geochronology using a frequency quintupled Nd:YAG based laser ablation system (λ = 213 nm) and quadrupole based ICP-MS, *J. Anal. At. Spectrom.*, *18*, 847–855.

Klepeis, K. A., M. L. Crawford, and G. Gehrels (1998), Structural history of the crystal-scale coast shear zone north of Portland Canal, southeast Alaska and British Columbia, *J. Struct. Geol.*, *20*, 883–904.

Kosler, J., H. Fonneland, P. Sylvester, M. Tubrett, and R.-B. Pedersen (2002), U-Pb dating of detrital zircons for sediment provenance studies—A comparison of laser ablation ICPMS and SIMS techniques, *Chem. Geol.*, *182*, 605–618.

Li, X.-H., X. Liang, M. Sun, Y. Liu, and X. Tu (2000), Geochronology and geochemistry of single-grain zircons: Simultaneous in-situ analysis of U-Pb age and trace element by LAM-ICP-MS, *Eur. J. Mineral.*, *12*, 1015–1024.

Li, X., X. Liang, M. Sun, H. Guan, and J. G. Malpas (2001), Precise $^{206}Pb/^{238}U$ age determination on zircons by laser ablation microprobe-inductively coupled plasma-mass spectrometry using continuous linear ablation, *Chem. Geol.*, *175*, 209–210.

Ludwig, K. R. (2001), Isoplot/Ex—A geochronological toolkit for Microsoft Excel, special publication, vol. 1a, 55 pp., Berkeley Geochronol. Cent., Berkeley, Calif.

Mank, A. J. G., and P. R. D. Mason (1999), A critical assessment of laser ablation ICP-MS as an analytical tool for depth analysis in silicate-based glass samples, *J. Anal. At. Spectrom.*, *14*, 1143–1153.

Mattinson, J. M. (2005), Zircon U-Pb chemical abrasion ("CA-TIMS") method: Combined annealing and multi-step partial dissolution analysis for improved precision and accuracy of zircon ages, *Chem. Geol.*, *220*, 47–66.

Outridge, P. M., W. Doherty, and D. C. Gregoire (1997), Ablative and transport fractionation of trace elements during laser sampling of glass and copper, *Spectrochim. Acta*, *52B*, 2093–2102.

Paces, J. B., and J. D. Miller Jr. (1993), Precise U-Pb ages of Duluth complex and related mafic intrusions, northeastern Minnesota: Geochronological insights to physical, petrogenetic, paleomagnetic, and tectonomagmatic processes associated with the 1.1 Ga midcontinent rift system, *J. Geophys. Res.*, *98*(B8), 13,997–14,014.

Premo, W. R. (1991), Isotopic ages and characteristics of the early Proterozoic Green Mountain magmatic arc, SE Wyoming-N. Colorado (abstract), *Geol. Soc. Am. Abstr. Program*, *20*, A73.

Schmitz, M. D., S. A. Bowring, and T. R. Ireland (2003), Evaluation of Duluth Complex anorthositic series (AS3) zircon as a U-Pb geochronological standard: New high-precision isotope dilution thermal ionization mass spectrometry results, *Geochim. Cosmochim. Acta*, *67*, 3665–3672.

Sylvester, P. J., and M. Ghaderi (1997), Trace element analysis of scheelite by excimer laser ablation-inductively coupled plasma-mass spectrometry (ELA-ICP-MS) using a synthetic silicate glass standard, *Chem. Geol.*, *141*, 49–65.

Tanner, S. D., L. M. Cousins, and D. J. Douglas (1994), Reduction of space charge effects using a three-aperture gas dynamic vacuum interface for inductively coupled plasma-mass spectrometry, *Appl. Spectrosc.*, *48*, 1367–1378.

Tiepolo, M. (2003), In situ Pb geochronology of zircon with laser ablation-inductively coupled plasma-sector field mass spectrometry, *Chem. Geol.*, *199*, 159–177.

Wiedenbeck, M., P. Alle, F. Corfu, W. L. Griffin, M. Meier, F. Oberli, A. Von Quadt, J. C. Roddick, and W. Spiegel (1995), Three natural zircon standards for U-Th-Pb, Lu-Hf, trace element and REE analyses, *Geostand. Newsl.*, *19*, 1–23.

Williams, I. S. (1998), U-Th-Pb geochronology by ion microprobe, *Rev. Econ. Geol.*, *7*, 1–35.